

Supplementary Material for:

Thermal Decomposition Reaction and a Comprehensive Kinetic Model of Dimethyl Ether

Zhenwei Zhao, Marcos Chaos, Andrei Kazakov, Frederick L. Dryer
Department of Mechanical and Aerospace Engineering
Princeton University
Princeton, NJ 08544
USA

DME Unimolecular Decomposition Calculations

Table S1. Rotational constants (B_A , B_B , B_C) and vibrational frequencies of species involved in DME decomposition reactions.

Species	Method	B_A , B_B , B_C (cm^{-1})	Frequencies (cm^{-1}) ^a
CH_3OCH_3	B3LYB/6-31G(d)	1.31, 0.33, 0.30	215.7 ^b , 241.8 ^b , 399.4, 919.9, 1091.3, 1128.2, 1161.6, 1167.4, 1228.5, 1425.3, 1449.5, 1457.2, 1458.3, 1466.7, 1487.6, 2855.3, 2869.8, 2900.4, 2903.5, 3008.0, 3009.6
CH_3O	B3LYB/6-31G(d)	5.24, 0.93, 0.92	712.3, 940.6, 1082.5, 1344.4, 1344.7, 1487.6, 2803.2, 2868.2, 2903.9
CH_3	B3LYB/6-31G(d)	9.51, 9.51, 4.76	434.9, 1373.8(2), 3017.5, 3185.1(2)

^a Frequencies at B3LYB/6-31G(d) level were scaled by a factor of 0.96.

^b These two vibration modes were replaced by two hindered rotors of CH_3OCH_3 .

Table S2. Energy (including ZPE correction) relative to CH_3OCH_3 for DME decomposition at 0 K.

Methods	$\text{CH}_3 + \text{CH}_3\text{O}$ (kcal/mol)
Nash & Francisco (1998) MP2/6-311G(2df,2p)//CCSD(T)/6-311++G(3df,3pd)	81.1
This Study G3B3//B3LYP/6-31G(d)	81.5
Experimental data (Benson 1956) [*]	81.1

^{*}Benson, S.W., J Chem Phys 1956, 25, 27-31.

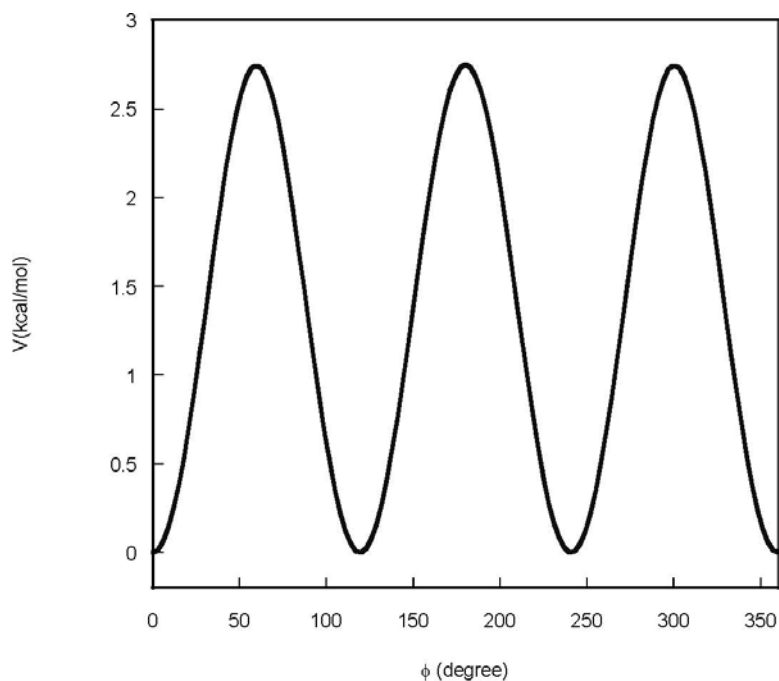


Fig. S1. Rotational potential of CH₃- rotors in DME used in density of states calculations.

Table S3. Recommended Arrhenius parameters for the forward rate constant expression $k=AT^n\exp(E_a/RT)$ for reaction $\text{CH}_3\text{OCH}_3 = \text{CH}_3 + \text{CH}_3\text{O}$ at different pressures for N₂ and Ar as bath gases.

Pressure (atm)	N ₂			Ar		
	<i>A</i>	<i>n</i>	<i>E_a</i>	<i>A</i>	<i>n</i>	<i>E_a</i>
1×10 ⁻¹⁰	6.3649E+49	-1.2938E+1	9.4701E+4	1.5340E+50	-1.3113E+1	9.4870E+4
0.01	1.0646E+50	-1.0723E+1	9.3505E+4	7.5320E+50	-1.1029E+1	9.3733E+4
0.1	8.2608E+46	-9.5549E+0	9.2944E+4	9.4439E+47	-9.9179E+0	9.3220E+4
1	1.6990E+42	-7.9536E+0	9.1807E+4	3.9113E+43	-8.3973E+0	9.2224E+4
10	6.2786E+35	-5.8914E+0	8.9712E+4	2.4956E+37	-6.3919E+0	9.0299E+4
100	7.2636E+28	-3.7476E+0	8.7001E+4	1.9533E+30	-4.1841E+0	8.7595E+4
∞	4.3790E+21	-1.5652E+0	8.3842E+4	4.3790E+21	-1.5652E+0	8.3842E+4

Comparing Predictions and Experimental Data for Flow Reactor Studies

Although discussed in detail in several previous articles, during the review process of this paper it was recommended further information be provided on the methods that our group utilizes for comparing experimental flow reactor data with plug flow predictions. Here we summarize the reasoning of and justifications for our approaches, so that in the future, perhaps readers can be referred to this single repository.

The Princeton Variable Pressure Flow Reactor (VPFR) is operated as a steady, adiabatic, and isobaric flow device and the residence time from the mixing point of the reactants to a sampling position along the tube axis can be varied in discrete increments. At the inlet of the reactor tube, fuel, diluted in nitrogen, is injected into a pre-mixed mixture of oxygen and nitrogen to obtain the desired equivalence ratio of reactants. Experiments are carried out under highly dilute conditions (using nitrogen). The mixing design at the injection location is such that the mixing time of reactants is small in comparison to the overall reaction residence time, from mixing to sampling locations. As in all similar flow reactor designs, there is a region subsequent to this mixing zone where radially uniform reacting conditions occur and (at least) the flow core simulates plug flow conditions. These issues have been experimentally verified in the VPFR. If these conditions are not met, for example, as in flow reactors that exhibit fully developed laminar flow velocity profiles, the region of reaction must be modeled as a two dimensional system, as described in [1]. In the homogeneous plug flow region downstream of the mixing region in the VPFR, the radial and axial diffusive terms in the conservation equations can be considered negligible, and the chemical composition with axial distance is a function of only chemical kinetics and flow velocity. Continuous sampling and quenching of a small portion of the reacting flow extracted at various axial locations along the homogenous reacting region (where velocity is known) provides the determination of species-temperature-time history information. The difficulty is that it is not possible to assure that reaction does not commence during the region in which mixing occurs. The hot mixing of individual reactant streams results in a region of inhomogenous concentration of initial species. In addition, chemical initiation can be perturbed by impurities in the reactants, catalytic interactions with mixing surfaces, and/or temperature transients accompanying the mixing of the independent reactant streams. The result is that the choice of the initial reaction time location (i.e. where conditions can be assumed to coincide to “homogenous” conditions and “zero” reaction, as exists at “ $t=0$ ” in plug flow predictions) is ill-defined.

The same difficulty is present in analyzing data from all flow reactors that mix reactants at temperatures near those to be studied. Some researchers assume that mixing times are negligible in comparison to the subsequent homogeneous reaction times, the mixed temperature is either measured or estimated by mixing rules, and the (potential) mixing effects on subsequent post induction reaction is assumed to be negligible (see for example the works of Glarborg and co-workers, e.g. [2]). This approach will be discussed in more detail below. Others have attempted to model the mixing phenomena as part of the predictive comparison, inclusive both temperature and composition history during the mixing process [3]. Noting that chemical induction processes are substantially influenced by the presence of reactive intermediates, others have varied the concentrations of these intermediates in the initial reactant composition to produce “matched” prediction and experimental reaction time profiles [4].

In an effort to avoid the above problem, other researchers perform flow reactor experiments by fully mixing “cold” reactants upstream of the reaction region, and then flowing the homogeneously mixed material into a heated region [5-8]. Frequently, these reactor designs cool down the entire reacting flow at the downstream end of the heated region to obtain chemical composition measurements. Reaction times are typically estimated from the measured volumetric flow rate and reactor volume. Boundary layer interactions in such devices necessitate assumptions about residence time relative to the core flow, surface reactions, and radial temperature non-uniformities that must exist in the heat up and cool-down regions. Frequently, a mean isothermal reaction temperature is assumed in computations, or the volumetric flow rate and estimated heat up and cool down temperature profiles are included in the modeling assumptions. Furthermore, such reactors often do not approximate plug flow conditions well throughout.

From our experience in developing flow reactor experimental techniques (e.g. [9, 10]) and in comparing numerical model results with flow reactor data [11-13], we have concluded that, in general, it is desirable to avoid matching computations and experiments at the initial point of mixing (as the beginning of reaction time), because in this vicinity, plug flow conditions are inexorably violated. For a dilute reacting system, in the plug flow region downstream of the location where mixing and reaction initiation take place, the theoretical model for mass, species and energy conservation (radial and axial diffusive terms in the governing equations are negligible, since the flow is developing and reactants are highly diluted in an inert carrier gas) results in a parabolic mathematical problem. Simply stated, any single arbitrary matching

condition of the calculated reaction profiles with the experimental data within the region where the above assumptions are experimentally approximated should be equivalent. Comparisons of calculations with measurements can then be performed upstream or downstream in time from this location as long as comparisons continue to be made only in contiguous regions where the mathematical assumptions remain experimentally well-approximated. As a result, the experimental regions can be modeled as a zero-dimensional, constant pressure system using computational programs such as SENKIN [14] or its equivalent. What remains is the choice of how to match the predictions and experiments within this context.

We prefer two approaches for defining the “matching condition” for computations with the experimental data. The methods are equivalent under the ideal conditions where only very low concentrations of intermediates (relative to reactant species) are produced in the experimental mixing region and the detailed kinetic computations are shown to result in limited sensitivities of the post induction chemistry to chemical perturbations by those intermediates present. The two methods are described below:

1. Time Shifting. In “time shifting” a matching criterion on the basis of a well-defined characteristic in the concentration of a particular measurable species (i.e. maximum gradient, maximum concentration, etc.) is used. This approach has been verified both numerically and experimentally elsewhere in the literature [11, 15-19]. In this procedure, the predicted species time histories are calculated using a zero dimensional approach with initial conditions defined by the initial reactant concentrations. The resulting computations are “shifted” such that a particular criterion (e.g. the 50% fuel disappearance) is matched and comparisons are then observed upstream and downstream of the matching point.

An excellent example of this approach is provided by the work of Yetter et al. [15] in their study of the CO/H₂O/O₂ system. Figure S2, compares the computed (using the present DME model) and experimental species time profiles for a near stoichiometric mixture of CO and O₂ with approximately 1% H₂O. In this figure the first experimental data point has been arbitrarily set to occur at t=0. By applying a 34.5 ms shift to the modeled data (in order to match the 50% fuel consumption point), excellent agreement is observed with measured profiles. By time shifting the computed profiles, comparisons can be performed without considering the chemical induction period during which the radical pool is established while fuel and oxidizer mix upstream of the sampling zone in the flow reactor. This mixing process, as discussed above, is obviously non-

ideal; however, as shown by Yetter et al. [15], disturbances in the radical pool formed during mixing only affect induction chemistry and have little or no lasting effect on the subsequent consumption of reactants; thus, validating the time-shifting approach. This is illustrated by Fig. S3 which shows model results under the same conditions of Fig. S2. Model calculations were stopped during the induction period (i.e. at 10 ms) and the concentrations of both the H and OH radicals were increased by an order of magnitude; the calculation was then restarted under these “perturbed” conditions. As seen in Fig. S3, the perturbations rapidly decay and after induction (after approximately 30 ms) there is virtually no difference between perturbed and unperturbed profiles. Considerable changes, however, do occur during chemical induction as shown by the CO₂ profile in Fig. S3. This is further supported by the fact that in order to match the 50% fuel consumption point of the data shown in Fig. S2, the perturbed profiles of Fig. S3 would have to be shifted by 30 ms rather than 34.5 ms, indicating a reduction of induction time caused by the perturbations.

Perturbations of induction time at other conditions and from other sources (such as back-mixing or catalytic surface reactions) can be large, causing considerable difficulty in interpreting flow reactor data as chemical ignition delay data [20]. Uncertainty analyses of flow reactor data [21] demonstrate this point. Zsély et al. [21] observed that uncertainties in the reaction initial conditions used in flow reactor simulations of carbon monoxide oxidation led to large uncertainties in the reaction time profiles, based on absolute reaction time scales. Their conclusion was that the particular flow reactor data provided poor constraints in validating the kinetic model. However, if experiment/model comparisons are made in a manner that ignores chemical induction processes and only compares post induction oxidation profiles, the uncertainties of species concentrations and temperature profiles provide strong constraints in validating the model. The use of time-shifting in the comparison accomplishes exactly this result (see comments in [21]).

Validation of the time shifting technique must be tested for every kinetic model and experimental system studied. Once validated, however, the methodology is straightforward and can be adopted in both local [18] and global [19] sensitivity analysis methods as an additional uncertainty. Moreover, Scire et al. [18, 19] also applied the technique over multiple species and conditions as a means of determining the “best” matching condition; uncertainties associated with the matching condition on the determination of elementary rate constants were also determined.

2. *Initialization.* This method (also referred to in some of our publications as “initial conditioning”) is more complex, but applies in all cases, including when, either experimentally, or computationally, reaction is observed to proceed such that significant quantities of the initial reactants are consumed and/or perturbations from the intermediates formed in the mixing region are observed to affect downstream, post-induction chemistry.

In the radially homogenous reaction region downstream of the mixing region, the initial conditions for the reaction are consistent with the initial reactants in terms of mass conservation, but the appropriate composition for comparing calculations with experimental results is no longer that of the initial reactant mixture. Li et al. [13], demonstrated and evaluated a methodology for defining the appropriate initial mixture conditions for matching the experimental and zero-dimensional computational predictions. In the particular ethanol pyrolysis experiments of Li et al. [13], ethanol decomposition to water and ethylene in the mixing region significantly perturbed the initial conditions appropriate to modeling the homogeneously mixed region downstream.

In most flow reactor experiments we perform, the measured stable species account for nearly all initially available carbon/oxygen mass and total carbon and oxygen conservation can be experimentally verified at each sampling location. Thus, it is reasonable to use the set of measured species mole fractions at a selected point downstream of the mixing region as the initial conditions for the predictions of the zero-dimensional experimental data downstream. The remaining issue is to define the corresponding local mole fractions of the species that are not available from the experimental data. Amongst the unknowns, there may be species of varying stability present in negligible amounts (in comparison to the total atom balances), including the very reactive species constituting the radical pool. On the other hand, once the radical pool is established, it is expected to respond quickly to the changes in the more slowly evolving species.

Based on this argument, we estimate the mole fractions of the unknown species by determining the quasi steady-state values constrained by available concentrations of the more stable (measured) species. This approach requires the solution of a non-linear algebraic system (specific to the chosen reaction mechanism) represented by $\dot{\omega}_i(P, T, \mathbf{x}^m, \mathbf{x}^u, x_{N_2}) = 0$, where $\dot{\omega}_i$ is the rate of production of an unknown species i obtained from detailed reaction mechanism, P the fixed total pressure, T the fixed temperature, \mathbf{x}^m fixed vector of mole fractions of the species available from experiments, \mathbf{x}^u vector of unknown species mole fractions. The mole fraction of

dilutant, x_{N_2} , is determined from the balance. The above system of equations is solved numerically using an in-house computer code and a two-step procedure. An approximation of the steady-state solution is obtained first, from a series of transient calculations performed with a stiff ordinary differential equation solver [22]. Then, the obtained approximation is further refined with a non-linear algebraic system solver based on Powell's hybrid method [23]. This method has been tested both computationally and experimentally, and the results obtained by using different extents of reaction for the matching location were found to be in excellent agreement with one another for both stable and radical species predictions in the regions downstream of the matching location [13]. In the accompanying paper, high pressure DME pyrolysis experiments (see Fig. 12 in the paper) show that reactions occur in the mixing zone upstream of the plug flow region that are substantial. Intermediates formed in this region affect the downstream pyrolysis rate essentially by changing the concentration of intermediates from those computed on the basis of plug flow computations using the initial reactant concentrations determined from flow rates to the mixing region. The initialization method was applied using the measured experimental concentrations reported in Fig. 12 at "t=0" to compute the complete species composition at t=0. The initialization concentrations used in the calculations reported in Fig. 12 are reported in Table S4.

The time shifting method is preferable to the initial conditioning method where applicable, both in terms of minimization of uncertainties, and ease of application. Either of these methods are preferable to attempting to compute multidimensional turbulent mixing for a chemically reacting system with detailed chemical kinetics in order to resolve the mixing zone itself (e.g., see [3]). In this case, substantial uncertainties are introduced by the assumptions required in CFD modeling of reacting flows in typical Reynold's number ranges found in experimental flow reactor studies. In essence, astute experimental configuration and careful interpretation of the region downstream lead to very small uncertainties in comparison to using either absolute time scale with or without including initial mixing and temperature transient effects in comparing experiments and computational predictions. In the present paper, we validated that the simple time-shifting approach could be applied without compromise for all of the predictive comparisons against flow reactor species-time histories for oxidation experiments, but as noted above, initialization methods was found to be appropriate for DME pyrolysis experiments.

The Assumption of Absolute Reaction Time from the Point of Mixing

We argue that the above techniques are preferable to assuming that the point of mixing is the equivalent to “time zero” in the computations and experiment. Glarborg and co-workers have typically applied this method in a majority of their flow reactor work (e.g. [2]). Initial reaction concentrations and the relative positions of sampling and mixing locations (reaction residence time) are held constant; the composition at the sampling point is reported as a function of the initial reaction temperature. In general, it is assumed that the mixing process occurs so rapidly that its effect on downstream kinetic observations is negligible. This result must be carefully tested, and in many cases, this assumption can result in significant uncertainties as to the veracity of the model/experiment comparison [24].

In some experiments reported in this and our earlier work on DME oxidation, we have also applied a similar analysis to investigate the low, negative temperature coefficient, and hot ignition characteristics of the oxidation. We refer to these types of experimental reactor data as “Reactivity Profiles” (e.g. Fig. 4 in accompanying paper). Experiments are performed with a fixed reactant composition and overall reaction time (based upon the flow time from the mixing point to the sampling location) and the chemical composition at the exit of the reaction zone is then determined as a function of the initial reaction temperature. The assumption made in comparing these data with computations is that mixing, catalytic processes, etc. in the mixing region have negligible effect on the time scales of the overall reaction. Surprisingly, the validation of using this technique is almost never questioned in the literature, nor is the methodology of time shifting compared with this approach.

Some simple calculations that utilize a perfectly stirred reactor (PSR) model to simulate the mixing effects are enlightening in terms of absolute time scale and time shifted comparisons of experimental data and predictions. A combined PSR-PFR model is used here to emulate the overall flow reactor, and the PSR model outlet concentrations are utilized as input initial conditions for the downstream plug flow reactor (PFR) model.

The steady-state algebraic mass conservation equation for a PSR can be given as:

$$\dot{m}(Y_i - Y_i^*) - \dot{\omega}_i M_i V = 0 \quad (1)$$

where, Y_i^* and Y_i are the inlet and out mass fractions. \dot{m} , $\dot{\omega}$ and M_i are the mass flow rate, molar rate of production and molecular weight of species i , respectively. V is the volume of the reactor. For a plug-flow reactor, the mass conservation equation is:

$$\frac{dY_i}{dx} - \left(\frac{\dot{\omega}_i M_i}{\rho u} \right) = 0 \quad (2)$$

where, x , ρ and u are axial distance, density and velocity, respectively. These PSR and PFR models are coupled such that the output species concentrations from the PSR become the initial species concentrations for the PFR.

Equation (1) can be expressed in terms of residence-time, τ_{psr} , as:

$$Y_i = Y_i^* + \left(\frac{\dot{\omega}_i M_i}{\rho} \right) \tau_{psr} \quad (3)$$

The composition of the species concentrations entering the flow reactor can be varied by changing the residence time of the PSR, τ_{psr} . The numerical simulations were performed using an in-house code built on the CHEMKIN II library [25].

The above PSR-PFR approach is similar to that used by Gokulakrishnan et al. [24] to illustrate how mixing can affect the interpretation of flow reactor data on an absolute reaction time scale basis. As an example, we compare here PSR-PFR calculations with the work of Bendtsen et al. [2] who performed a series of flow reactor experiments to study NO sensitization on CH₄ oxidation. The experiments were carried out in a flow reactor under isothermal conditions between 800 and 1300 K, and stable species were measured in the exhaust gas. Figure S4 shows reported CO, CO₂, and CH₄ measurements, for an inlet gas composition of 2276 ppm CH₄, 3.69 % O₂ and 4 % H₂O in N₂ in the absence of NO. During the oxidation of CH₄, considerable amounts of CO were formed between 1125 and 1225 K. Figure S4 also shows the modeling results (using GRI 3.0 [26]) generated from a plug-flow simulation without considering the effect of mixing at the inlet to the reactor.

Figure S5 depicts the CO time-history profile calculated using a PSR-PFR simulation for the experimental conditions specified in Fig. S4. Figure S5 shows CO profiles for PSR residence times of 0, 15, 30, and 45 ms, compared to the overall reaction time scale of 249.6 sK / 1140 K = 218.95 ms. As the PSR residence time is increased, the CO formation is accelerated in terms of absolute time; however, the CO profile itself remains unchanged. For example, the CO profile for 30 and 45 ms can exactly be over-layed by time-shifting. Figure S6 shows the calculated CO concentration profiles at the exit of the PFR as a function of PSR residence time for 1130, 1140 and 1150 K. It is clear from Fig S6 that small mixing time-scales in the upstream of the flow reactor can have a dramatic impact on the exit plane CO concentration. For example, at 1140 K,

a PSR residence time of 20 ms results in increasing the CO exit plane concentration by over an order of magnitude from the value calculated when mixing is instantaneous (i.e. $\tau_{\text{psr}}=0$).

The above discussion illustrates two important points. It is shown that if time shifting is verified to apply, the features of the CO profiles themselves are constrained by the chemical kinetic mechanism, while the absolute time scales at which these profiles occur are strongly influenced by mixing effects (which impact induction chemistry), consistent with the work of Yetter et al. [12, 15].

The second important point is that comparing experimental data and predictions using absolute time scales from the point of mixing needs to be carefully evaluated in terms of assessing mixing effects on the overall measurements. For the DME “reactivity” experiments presented in the accompanying paper (i.e. Fig. 4), such an assessment is shown in Fig. S7. PSR-PFR calculations similar to those described above were performed by varying the PSR residence time between 0 and 0.5 s (compared to the overall flow reactor residence time of 1.8 s). It is evident that even for a PSR residence time of 0.5 s (which is estimated to be an order of magnitude larger than the expected mixing time in the VPFR), calculated profiles are marginally different than for a PSR residence time of zero. In this case, the use of an absolute residence time is found to be a valid methodology for comparing model and experimental results.

References

1. Lee, J.C.; Yetter, R.A.; Dryer, F.L.; Tomboulides, A.G.; Orszag, S.A. *Combust Sci Tech* 2000, 159, 199-212.
2. Bendtsen, A.B.; Glarborg, P.; Dam-Johansen, K. *Combust Sci Tech* 2000, 151, 31-71.
3. Schmidt, C.C.; Bowman, C.T. *Combust Flame* 2001, 127, 1958-1970.
4. Hunter, T.; Wang, H.; Litzinger, T.; Frenklach, M. *Combust Flame* 1994, 97, 210-224.
5. Hardy, J.E.; Lyon R. *Combust Flame* 1980, 39, 317-320.
6. Dean, A.M.; Hardy J.E.; Lyon, R. *Proc Combust Inst* 1980, 19, 97-105.
7. Wu, Y.-G.; Lin, Y.-F. *Combust Flame* 2004, 137, 376-402.
8. Sheng, Y.S.; Dean, A.M. *J Phys Chem A* 2005, 108, 3772-3783.
9. Crocco, L.; Glassman, I.; Smith, I.E. *Jet Propul* 1957, 27, 1266-1267.

10. Dryer, F.L. Ph.D. Thesis; Department of Aerospace and Mechanical Sciences, Princeton University, Princeton, NJ, 1972. Report Number AMS-T-1034.
11. Yetter, R.A. Ph.D. Thesis; Department of Mechanical and Aerospace Engineering, Princeton University, Princeton, NJ, 1985. MAE Report No. 1703-T.
12. Yetter, R.A.; Dryer, F.L.; Rabitz, H. Combust Flame 1985, 59, 107-133.
13. Li J.; Kazakov, A.; Dryer, F.L. Int J Chem Kinet 2001, 33, 859-867.
14. Lutz, A.E.; Kee, R.J.; Miller, J.A. Technical Report SAND87-8248; Sandia National Laboratories, 1987.
15. Yetter, R.A.; Dryer, F.L.; Rabitz, H. Combust Sci Tech 1991, 79, 129-140.
16. Held, T.J. Ph.D. Thesis; Department of Mechanical and Aerospace Engineering, Princeton University, Princeton, NJ, 1993.
17. Scire, J.J. Ph.D. Thesis; Department of Mechanical and Aerospace Engineering, Princeton University, Princeton, NJ, 2001. MAE Report No. 3101-T.
18. Scire, J.J.; Yetter, R.A.; Dryer, F.L. Int J Chem Kinet 2000, 33, 75-100.
19. Scire, J.J.; Yetter, R.A.; Dryer, F.L. Int J Chem Kinet 2001, 33, 784-802.
20. Chaos, M.; Dryer, F.L. Combust Sci Tech 2007, in press.
21. Zsély, I.Gy.; Zádor, J.; Turányi, T. Proc Combust Inst 2005, 30, 1273-1281.
22. Brown, N.; Byrne, G.D.; Hindmarsh, A.C. SIAM J Sci Stat Comput 1989, 10, 1038-1051.
23. Powell, M.J.D. in Numerical Methods for Nonlinear Algebraic Equations; Rabinowitz, P. (Ed.); Gordon and Breach: New York, 1970.
24. Gokulakrishnan, P.; Kazakov, A.; Dryer, F.L. 3rd Joint Meeting of the U.S. Sections of the Combustion Institute, University of Illinois at Chicago, Chicago, IL, March 16-19, 2003.
25. Kee, R.J.; Rupley, F.M.; Miller, J.A. Technical Report SAND89-8009; Sandia National Laboratories, 1989.
26. Smith, G.P.; Golden, D.M.; Frenklach, M.; Moriarty, N.W.; Eiteneer, B.; Goldenberg, M.; Bowman, C.T.; Hanson, R.K.; Song, S.; Gardiner, Jr., W.C.; Lissianski, V.V.; Qin, Z. http://www.me.berkeley.edu/gri_mech/.

Tables

Table S4. Initialization composition used in the model-experiment comparisons presented in Fig. 12 of accompanying paper. Only those species with concentrations larger than 0.1 ppm are reported.

Species	Mole Fraction
CH ₃ OCH ₃	1.2450×10^{-3}
CH ₄	1.9121×10^{-4}
CO	1.2769×10^{-4}
CH ₂ O	1.5470×10^{-4}
C ₂ H ₆	1.3700×10^{-5}
CH ₃	1.0133×10^{-7}
H ₂ O	2.2109×10^{-4}
N ₂	9.9802×10^{-1}
O ₂	1.9894×10^{-5}
CH ₃ OH	2.1209×10^{-6}
CH ₃ HCO	1.0496×10^{-7}

Figures

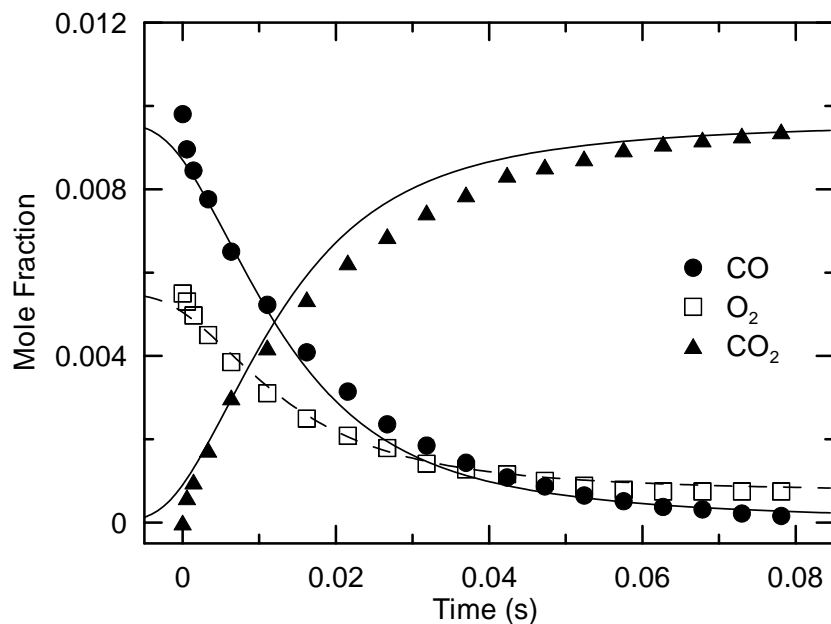


Figure S2. Species concentration profiles for a CO/H₂O/O₂/N₂ mixture (0.96/0.56/0.55/97.93 %) at 1033 K and 1 atm. Symbols represent experimental measurements [15]; lines are model predictions, dashed lines correspond to open symbols. Model profiles have been shifted by -34.5 ms to match the 50% CO consumption point.

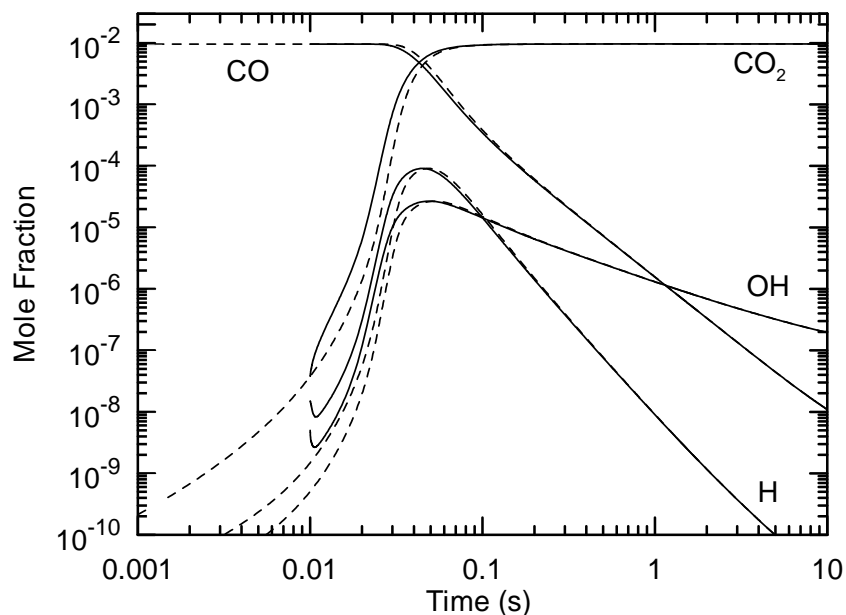


Figure S3. Species profiles with order-of-magnitude perturbations of H and OH concentrations at 10 ms. Initial conditions are those listed in Fig. S2. Dashed lines are the unperturbed profiles shown in Fig. S2, solid lines represent the perturbed profiles.

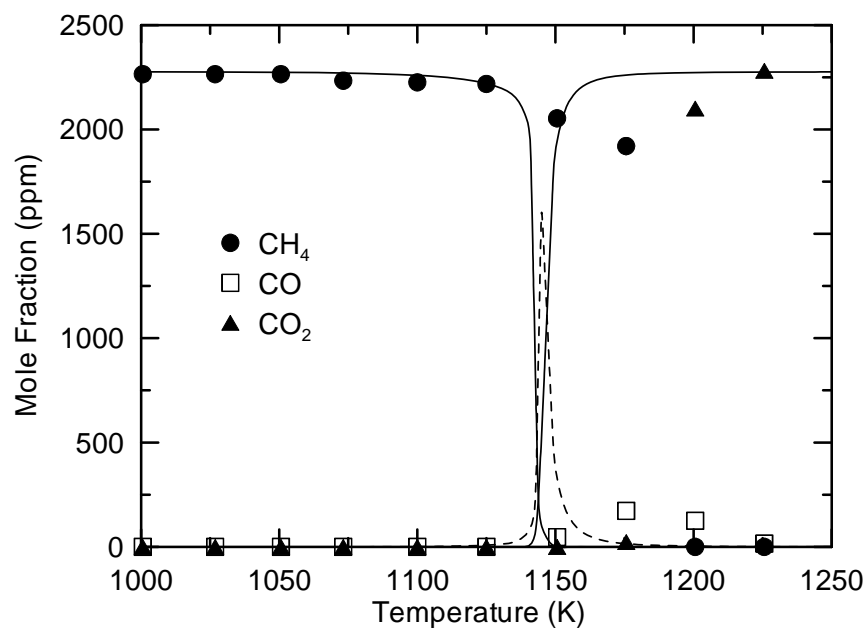


Figure S4. Concentrations of CO, CO₂, and CH₄ measured at the exhaust of an isothermal, tubular flow reactor during the oxidation of CH₄ from Bendtsen et al. [2]. The inlet gas composition to the reactor was 2276 ppm CH₄, 3.69 % O₂ and 4 % H₂O in N₂. The symbols denote experimental measurements and the lines represent plug-flow modeling results. The dashed line corresponds to open symbols. Residence time = 249.6 sK/T.

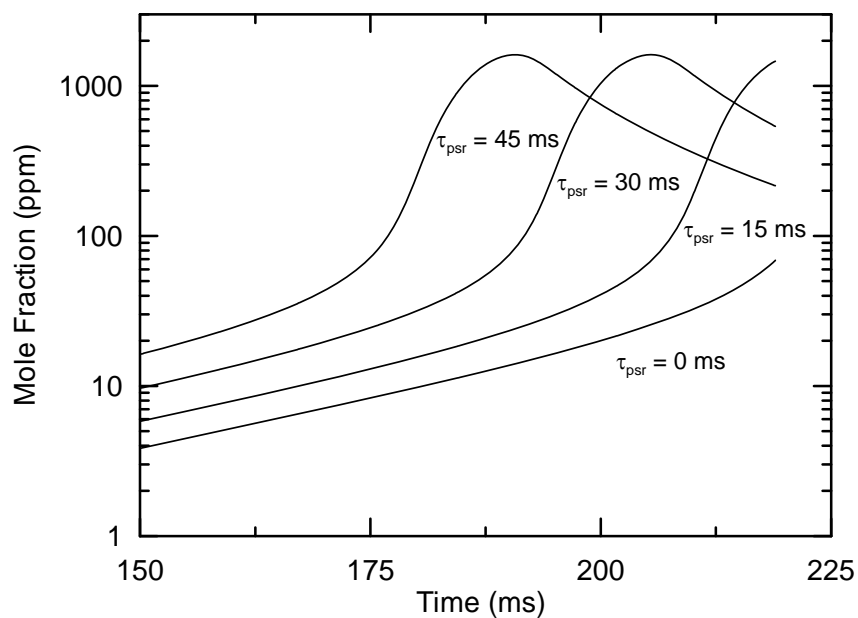


Figure S5. Calculated CO time-history profiles different τ_{psr} values at 1140 K for the experimental conditions specified in Fig. S4.

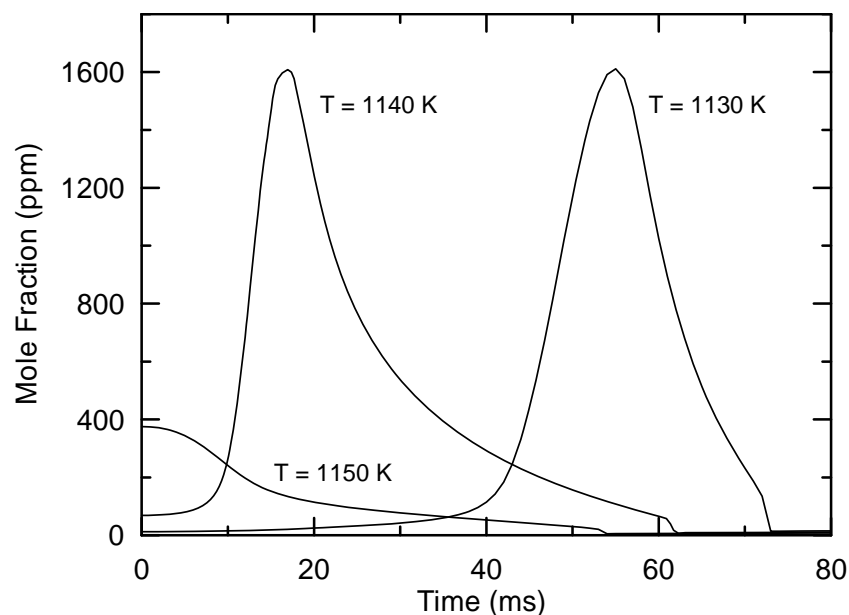


Figure S6. PSR-PFR numerical simulation of CO profiles at the PFR exit for various temperatures as a function of PSR residence time, τ_{psr} , for the experimental conditions specified in Fig. S4.

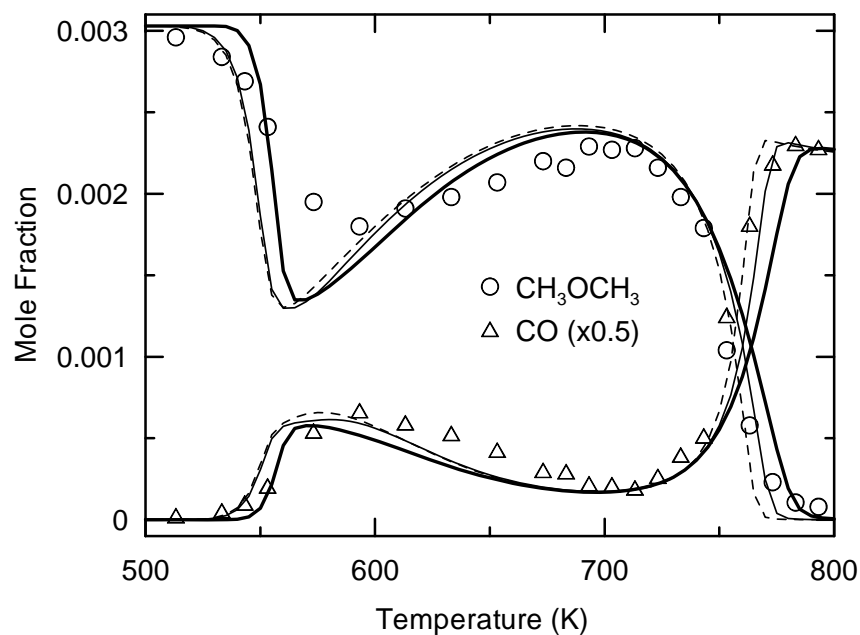


Figure S7. Computed DME and CO profiles in a variable pressure flow reactor ($P = 12.5$ atm, 3030 ppm DME, $\phi = 1.19$, in balance N_2 , residence time = 1.8 s) compared with experiments (see Fig. 4 in paper). Calculations were performed using a PSR-PFR combination (see text). Bold solid lines are results assuming a PSR residence time (τ_{psr}) of 0 s, solid lines are results for $\tau_{psr} = 0.25$ s, and dashed lines are results for $\tau_{psr} = 0.5$ s.